

Crystallisation kinetics and density profiles in ultra-thin hafnia films

Crystallisation and structure of HfO₂ films

A. van der Lee^{1,a}, J. Durand¹, D. Blin^{2,b}, Ph. Holliger³, and F. Martin³

¹ Institut Européen des Membranes, UM-II cc047, 34095 Montpellier Cedex 5, France

² ASM France, 1025 rue Henri Becquerel, 34036 Montpellier Cedex 1, France

³ CEA-DRT-LETI, 17 rue des Martyrs, 38054 Grenoble Cedex 9, France

Received 8 March 2004

Published online 29 June 2004 – © EDP Sciences, Società Italiana di Fisica, Springer-Verlag 2004

Abstract. Crystallisation onset temperatures as a function of chlorine contamination have been determined by grazing incidence diffraction on as-deposited ultra-thin HfO₂ films grown by Atomic Layer Deposition. The onset temperatures are positively correlated with chlorine content, suggesting defect-hindered crystallisation kinetics. Density profiles have been deduced by reflectometry measurements and a model independent analysis scheme. It is shown that the HfO₂/SiO₂-Si interface is electronically denser than the bulk of the HfO₂ film.

PACS. 68.35.Ct Interface structure and roughness – 68.55.Jk Structure and morphology; thickness; crystalline orientation and texture – 64.70.Nd Structural transitions in nanoscale materials

1 Introduction

Thin HfO₂ films have been extensively studied because of their potential applications as high-*k* gate dielectric materials in CMOS transistors. These high-*k* materials could replace SiO₂ as the material of choice for silicon microelectronics, since they have physico-chemical properties that are close to those of SiO₂ with the advantage of having a much higher permittivity [1]. It is generally accepted that an extremely thin, but controlled underlayer of SiO₂ is needed to enlarge the structural quality of the high-*k* layer and the electrical quality of the interface. The chemical nature of the HfO₂/SiO₂ interface is still not clear; it certainly depends on the nature of the deposition process and on the deposition parameters.

In this paper several aspects of the HfO₂/SiO₂ interface in HfO₂ layers with a thickness of technological interest (3.5 nm) will be addressed. Firstly, the influence of residual chlorine on the crystallisation onset temperature is investigated. It has been proven that residual chlorine is present at the HfO₂/SiO₂ interface as a result of incomplete chemical reaction in the early stage of the deposition from HfCl₄ in the Atomic layer Deposition (ALD) process [2]. Crystallisation of the dielectric layer during

thermal treatments needed in the final CMOS processing, is reported to enhance leakage currents [3], although other reports show that even crystalline films could have rather good electrical properties [4]. Crystallisation studies of thin films of HfO₂ and ZrO₂ have been reported before, but they were done on either much thicker films than in this study or with a much less accurate temperature scheme than was employed here [4–6]. The influence of the chlorine impurities has never been investigated to our knowledge. Secondly, the electronic density profile of typical ultra-thin films is determined by X-ray reflectometry (XRR). Variations in an otherwise constant profile can be correlated to chemical profiles as determined by Secondary Ion Mass Spectroscopy (SIMS).

2 Sample preparation

HfO₂ films with a thickness of about 3.5 nm were deposited in a Pulsar® 2000 ALCVDTM reactor from ASM Microchemistry Ltd on low doped, p-type, 8" oxidized Si(100) substrates. The silicon surface was prepared using an ozone solution leading to a 0.7 nm thick SiO₂ layer. Each sample was first brought in the introduction chamber at 10⁻³ Torr and subsequently transferred to the reaction chamber. The two precursor vapours HfCl₄ and H₂O were then successively introduced in the form of short pulses,

^a e-mail: avderlee@univ-montp2.fr

^b Present address: Jusung Europe, 12 boulevard Gambetta, BP 371, 38014 Grenoble, France

separated by 2 second pulses of N_2 in order to evacuate the excess precursor vapour and gaseous by-products of the reaction. The pressure in the reaction chamber was approximately 1 Torr. Deposition temperature and H_2O pulse time were varied in the range of 300 °C to 350 °C and 50 ms to 3000 ms, respectively. The $HfCl_4$ pulse time was fixed at 50 ms. After the last cycle and a post-stabilisation time the sample was back-transferred to the introduction chamber and recovered at ambient pressure. The sample was hereafter brought to the high-temperature chamber of the diffractometer without any further precautions.

3 Grazing incidence X-ray diffraction and complementary techniques

X-ray investigations of extremely thin films are best done under grazing incidence conditions in order to enhance the amount of irradiated matter and a fast detector is required to follow the crystallisation process on a time scale of minutes. For the present measurements a PanAnalytical X'pert-Pro diffractometer was used, equipped with an ultrafast X'celerator detector and an Anton Paar HTK-1200 oven operating in a N_2 atmosphere. Cu $K-L_{3,2}$ X-rays were used with a Ni-filter in the incident beam. After a scan at ambient temperature, the sample was heated at a speed of 10 °C/min to 390 °C and then at 7 °C/min in intervals of 10 °C to the next temperature where a 5 minutes scan was done under grazing incidence conditions ($\theta_i = 0.5^\circ$). Samples with different chlorine concentrations were investigated. The final crystallisation onset temperature T_c was estimated by a linear extrapolation to zero peak area from the observed peak areas at each temperature. Figure 1 shows an example with different measurements between ambient temperature and 500 °C. Whereas at 410 °C there is no sign of crystallisation, at 420 °C – several minutes later – roughly half of the film is crystallised. At 500 °C the film is fully crystallised. Full crystallisation, considered as the temperature at which the peak area did not change anymore, could also be reached by keeping the temperature at 420 °C for a while. In another experiment the film was left approximately 10 °C below T_c and successive scans were performed until crystallisation set in after roughly 50 minutes. Scans of wider intervals showed only the principal (-111) peak of the monoclinic phase. Cubic, orthorhombic and tetragonal phases have been reported as well for ALD-deposited thin films of HfO_2 and ZrO_2 , but in general only for higher substrate temperatures [7,8]. It is noted that in the bulk they are, unlike the monoclinic phase, only formed at high temperatures and/or high pressures, so in the thin film they should be considered as quenched metastable phases. The crystallite size determined from the full width at half maximum of the principal peak using the Scherrer equation (corrected for instrumental resolution) is approximately 4.5 nm, which can be considered, in view of the approximate character of the Scherrer equation, to be equal to the film thickness.

Figure 2 shows that T_c positively depends on the chlorine concentration. SIMS-profiles were determined using

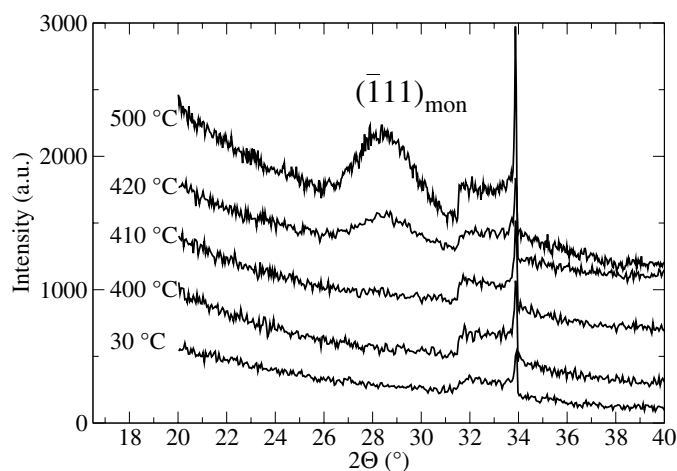


Fig. 1. Grazing incidence diffraction for one of the samples at different temperatures. The signal around $2\theta = 34^\circ$ is due to the particular grazing incidence geometry and could be due to sample holder and/or peaks from the substrate observed in grazing incidence geometry ($\lambda/2$ contamination).

a Cameca IMS 5F apparatus on a $200 \times 200 \mu m^2$ surface area on 8 nm thick samples grown under similar conditions, since the 3.5 nm thick samples did not give accurately enough results. The chlorine concentrations in the bulk of the 3.5 and 8 nm thick samples were assumed to be the same and small with respect to the concentrations at the interfaces. Cs^+ primary ions were used for Cl depth profiling with an impact energy of 1 keV and an angle of incidence of 50° . Positive secondary ion signals MCs_2^+ (where $M = O, Cl$ and Si) were monitored with a depth resolution of about 1 nm [9]. The Cl atomic concentrations were calibrated with a ^{35}Cl -implanted (energy: 20 keV, dose: 10^{16} at cm^{-2}) 50 nm thick HfO_2 sample and a ^{35}Cl -implanted (energy: 20 keV, dose: 10^{15} at cm^{-2}) Si substrate. The profiles obtained (see inset of Fig. 2) show that chlorine is predominantly present at the HfO_2/SiO_2 interface [10]. In addition, a Cl diffusion towards the surface sample is systematically observed for all the profiles. The duration of the H_2O pulse time proves thus to be an effective means to control the chlorine contamination [2]. Chlorine sites can not be considered as preferential nucleation sites where the growth of (amorphous) HfO_2 starts. Instead a perturbed region around the chlorine sites is created, in which there are less OH groups. This limits the dehydroxylation process during growth, so that less Hf-O-Hf bridges are formed. An extended network of such bridges is expected to favour crystallisation. Since the films are so extremely small the perturbed (i.e. Hf-O-Hf poor) regions can extend to the surface of the film, therefore preventing lateral proliferation of crystalline domains. It can therefore be expected that the influence of chlorine contamination on T_c is less for thicker films. Chlorine outdiffusion is not expected to play a role, since this becomes important only at temperatures above 1000 °C [11]. Figure 3 shows a dark-field Transmission Electron Microscopy (TEM) plane view of the initial phase of crystallisation in one of the thin HfO_2 films that was recovered from the high-temperature

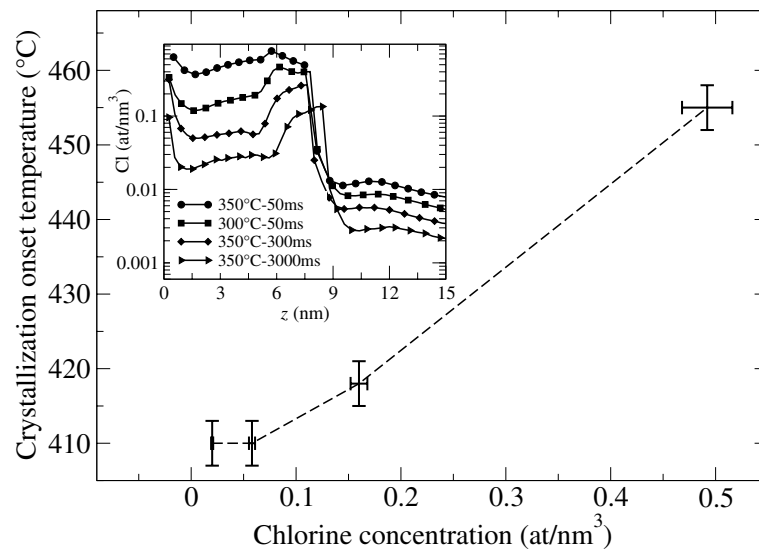


Fig. 2. Crystallisation onset temperature as a function of chlorine concentration in ultrathin HfO_2 films. The dashed line only serves as a guiding line for the eye. The inset gives the SIMS-derived Cl profiles for four slightly thicker samples, grown under the same experimental conditions.

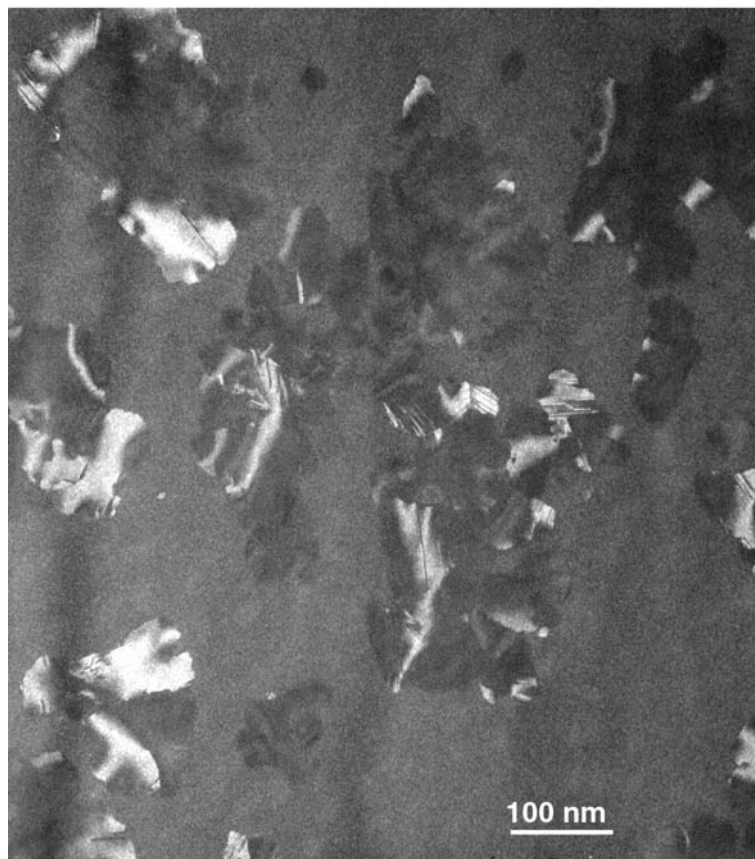


Fig. 3. TEM plane view of the initial phase of crystallisation in one of the 3.5 nm thick HfO_2 samples.

chamber just after crystallisation set in. The grey background corresponds to the amorphous matrix, whereas the different brighter areas correspond to crystallised regions in different orientations with respect to the incident beam.

4 Grazing incidence X-ray reflectometry

Additional insight in the $\text{HfO}_2/\text{SiO}_2$ interface can be obtained by high-resolution X-ray reflectometry (XRR) experiments. XRR probes the density profile normal to the surface and is relatively easy to perform. Data analysis however is not straightforward: usually the layer is divided into parallel sublayers, each layer having its own thickness, density, and interfacial roughness ('slice fitting' or 'optical matrix method'). The density is normally the electronic density; if the mass density is fitted then the composition is a refinable parameter as well. Fitting the data in this way is limited to at most three layers, and is strongly dependent on the initial model. Fitting the data of ultra-thin HfO_2 has its own difficulties. Due to the strong density contrast between the 3.5 nm HfO_2 layer and the Si substrate on the one hand and the very low density contrast between the substrate and the 0.7 nm thick SiO_2 layer on the other hand, the latter layer is invisible in the XRR experiment; the presence or absence of such a layer will not significantly change the reflectivity curve. It is noted that XRR experiments have been performed before on hafnia layers, in some cases also on layers with a thickness in the same range (3–4 nm) as in this paper [10,12]. The conclusions that are drawn, however, cannot always be warranted by the data. Lysaght et al. [10] presented a four-layer model that included several non-physical aspects, such as a 0.41 nm thick SiO_2 layer that is clearly invisible in the experiment. Another point of his model is a 0.35 nm thick low density HfO_2 (57% of bulk) layer at the surface, combined with a surface roughness of 0.89 nm which is clearly incompatible with the layer thickness. In view of these problems a quasi model-independent approach (Distorted Wave Born Approximation (DWBA) method) [13]) has been chosen to fit the reflectivity data, which gives the best least-squares density profile compatible with the data, and much less biased by the starting point than is the case using the optical matrix method. The starting point is a constant density across the film; the algorithm looks then for the deviations with respect to this constant density by using the DWBA expression for the reflectivity, resulting in a electronic density profile of the film. With this method a very good agreement between calculated and measured reflectivity data could be obtained. An independent check of the results was obtained using alternative and mathematically completely different methods, such as Sanyal's Born Approximation (BA) method [14] or the phaseless inverse scattering method [15]. These methods gave qualitatively the same results, but should be considered a bit less accurate than the DWBA method, because of the more approximate character of the BA compared with the DWBA, and of the non-negligible absorption in the case of the phaseless inverse scattering method.

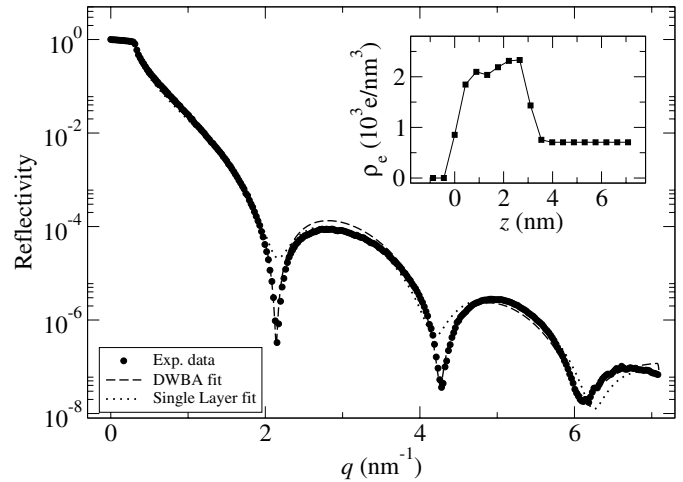


Fig. 4. Reflectivity of a 3.5 nm thick HfO_2 film and (inset) the density profile used in the DWBA-fit.

The measurements were performed using a Bruker D5000 diffractometer with $\text{Cu } K\text{-}L_{3,2}$ radiation and a graphite monochromator in the secondary beam. Reflectivity data were collected with a special reflectivity stage consisting of a knife edge in the center of the goniometer that cuts the beam to a 15 micron height. The width of the beam was 15 mm. In this way exploitable data could be recorded up to $q = 7.1 \text{ nm}^{-1}$ which is equivalent to a real space resolution of $\Delta z = 0.88 \text{ nm}$, a better resolution than has been reported before. The off-specular scattering was measured as well and used to subtract the background from the measured specular signal in order to obtain the true specular reflectivity. Figure 4 shows the experimental data and the calculated reflectivities using either a one-layer model or a model-independent fitting method. Other films, grown under different conditions, with different chlorine concentrations, yielded similar reflectivity curves. The one-layer model is clearly not adequate enough to explain the experimental data; the DWBA-based model (see the profile in the inset) describes much better the fringe amplitudes. The profile suggests that there is a region of enhanced electronic density at the $\text{HfO}_2/\text{SiO}_2$ interface, whereas the electronic density of the 'bulk' of the film is approximately 87% of that in the bulk of monoclinic HfO_2 (2540 e/nm^{-3}). It is noted that an enhanced electronic density at the $\text{HfO}_2/\text{SiO}_2$ interface was proposed earlier by Lysaght et al. [10] but this was based on a questionable model-dependent four-layer fitting method (*vide supra*). In view of the similarities between the density profiles of Figure 4 and the inset of Figure 2 it is tempting to ascribe the enhanced electronic density at the $\text{HfO}_2/\text{SiO}_2$ interface to the presence of Cl, but the chlorine concentration is far too small compared to the bulk HfO_2 density. The presence of a silicon-rich hafnium silicate-like phase have been proved to exist at the $\text{HfO}_2/\text{SiO}_2$ interface [16], but it should be noted that the electronic density of bulk HfSiO_4 is 1832 e/nm^{-3} . Therefore we think that the enhanced density at the $\text{HfO}_2/\text{SiO}_2$ interface must be due

to a particular rather dense structural intermixing of possibly amorphous $\text{Hf}_y\text{Si}_z\text{O}_4$ and SiO_x .

The surface region is another point of interest. The surface roughness can be estimated from Figure 4 or eventually from the parameters from the one-layer model fit. The value found for these films is in general between 0.35 and 0.4 nm. Off-specular scattering is very low for these films, suggesting that the apparent roughness is only partly due to physical rms roughness, and that the HfO_2 density is slowly falling off from the bulk to the outer surface. This is not similar to Lysaght's low density HfO_2 layer [10], but should rather be considered as a diffuse interface with only very low physical rms roughness where the density gradually changes to zero. AFM images, which are only sensitive to the physical rms roughness, give indeed smaller roughness values (approximately 0.2 nm).

5 Conclusions

In conclusion, by grazing incidence X-ray diffraction we have determined crystallisation onset temperatures as a function of chlorine contamination in ultrathin HfO_2 layers. Perturbed areas around the chlorine sites at the $\text{SiO}_2/\text{HfO}_2$ interface hinder the crystallisation of the amorphous material. XRR measurements have shown the presence of a relative dense layer at the $\text{SiO}_2/\text{HfO}_2$ interface. This dense transition layer is a complicated mixture of silicon oxide, hafnium silicate, and a relatively large amount of chlorine contamination sites.

Dr. A.-M. Papon (CEA-DRT/LETI-DPTS, Grenoble) is thanked for providing the TEM-image.

References

1. G.D. Wilk, R.M. Wallace, J.M. Anthony, *J. Appl. Phys.* **89**, 5243 (2001)
2. D. Blin, N. Rochat, G. Rolland, P. Holliger, F. Martin, J.-F. Damlencourt, T. Lardin, P. Besson, S. Haukka, M.-N. Séméria, *Proc. 203rd Meeting Electrochem. Soc., Paris (2003)*
3. J. Aarik, A. Aidla, H. Mändar, T. Uustare, *J. Cryst. Growth* **220**, 105 (2000)
4. M.-Y. Ho, H. Gong, G.D. Wilk, B.W. Busch, M.L. Green, P.M. Voyles, D.A. Muller, M. Bude, W.H. Lin, A. See, M.E. Loomans, S.K. Lahiri, P.I. Räisänen, *J. Appl. Phys.* **93**, 1477 (2003)
5. C. Zhao, G. Roebben, H. Bender, E. Young, S. Haukka, M. Houssa, M. Naili, S.D. Gendt, M. Heyns, O. Van Der Biest, *Microelectronics Reliability* **41**, 995 (2001)
6. S. Stemmer, Z.Q. Chen, W.J. Zhu, T.P. Ma, *J. Microscopy* **210**, 74 (2003)
7. J. Aarik, A. Aidla, A.-A. Kiisler, T. Uustare, V. Sammelselg, *Thin Solid Films* **340**, 110 (1999)
8. J. Aarik, A. Aidla, H. Mändar, T. Uustare, K. Kukli, M. Schuisky, *Appl. Surf. Science* **173**, 15 (2001)
9. Ph. Holliger, F. Laugier, J.C. Dupuy, *Surf. Interface Anal.* **34**, 472 (2002)
10. P.S. Lysaght, P.J. Chen, R. Bergmann, T. Messina, R.W. Murto, H.R. Huff, *J. Non-Crystalline Sol.* **303**, 54 (2002)
11. S. Ferrari, G. Scarel, C. Wiemer, M. Fanciulli, *J. Appl. Phys.* **92**, 7675 (2002)
12. S. Ferrari, M. Modreanu, G. Scarel, M. Fanciulli, *Thin Solid Films* **450**, 124 (2004)
13. M.K. Sanyal, J.K. Basu, A. Datta, S. Banerjee, *Europhys. Lett.* **36**, 235 (1996)
14. M.K. Sanyal, S. Hazra, J.K. Basu, A. Datta, *Phys. Rev. B* **58**, 4258 (1998)
15. A. van der Lee, *Eur. Phys. J. B* **13**, 755 (2000)
16. O. Renault, D. Samour, J.-F. Damlencourt, D. Blin, F. Martin, S. Marthon, N.T. Barrett, P. Besson, *Appl. Phys. Lett.* **81**, 3627 (2002)